SECOND EDITION

Intermolecular & Surface Forces

JACOB ISRAELACHVILI

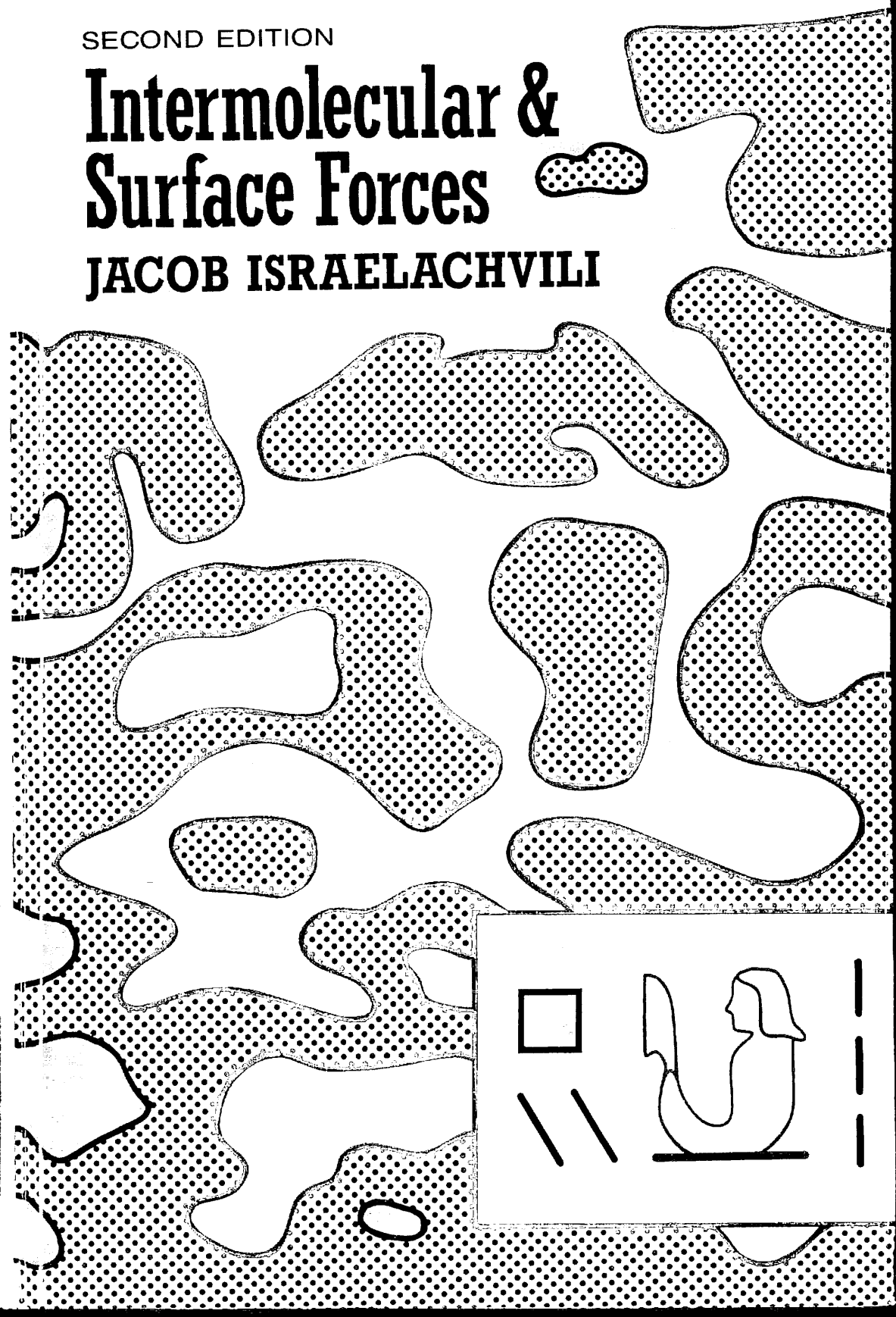

them into a liquid or solid (see Table 6.1, Chapter 6). It is for this reason that the thermal energy $\sim\frac{3}{2}kT$ can be used as a standard reference for gauging the cohesive strength of an interaction potential, though it is essential to note that this indicator, and Trouton's rule, are valid only because of the particular value of the atmospheric pressure on the earth's surface. This pressure determines that a gas molecule will occupy a volume of about 4×10^{-20} cm^3 at or near STP, which is needed for deriving Eqs (2.24)–(2.26).

It is also worth mentioning that the notion that molecules go into the vapour phase because of the kinetic energy $\frac{3}{2}kT$ they acquire is not correct. Their kinetic energy does not disappear in a liquid or solid; the molecule's motion is merely restricted to a narrower region of space around a potential-energy minimum. The average translational kinetic energy of a molecule is $\frac{3}{2}kT$ irrespective of whether it is in the gas, liquid or solid state. We shall not here consider the very complex energies associated with rotational and vibrational states of molecules in solids, liquids and gases, which would take us outside the scope of this book.

So far the Boltzmann distribution has been used to find the spatial or density distribution of molecules in different regions of a system. The Boltzmann distribution can also be used to determine the *orientational distribution* of molecules. For example, if the pair potential also depends on the mutual orientation of two anisotropic molecules, i.e., if $w(r)$ is also angle-dependent so that it may be written as $w(r, \theta)$, then the angular distribution of two molecules at a fixed distance r apart will be

$$X(\theta_2) = X(\theta_1) \exp\left(- \frac{w(r, \theta_2) - w(r, \theta_1)}{kT} \right), \tag{2.28}$$

and here again the factor kT appears as a convenient energy unit, but this time it appears for the strength of orientation-dependent interactions needed to align molecules mutually (e.g., solvent molecules around a dissolved solute molecule, discussed in Chapters 4 and 5).

2.6 CLASSIFICATION OF FORCES

Intermolecular forces can be loosely classified into three categories. First, there are those that are *purely electrostatic* in origin arising from the *Coulomb force* between charges. The interactions between charges, permanent dipoles, quadrupoles, etc., fall into this category. Second, there are *polarization forces* that arise from the dipole moments *induced* in atoms and molecules by the electric fields of nearby charges and permanent dipoles. All interactions in

Type of interaction		Interaction energy $w(r)$
Covalent, metallic	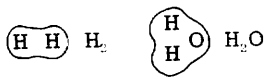	Complicated, short range
Charge–charge	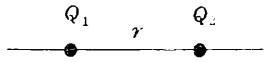	$Q_1Q_2/4\pi\varepsilon_0 r$ (Coulomb energy)
Charge–dipole	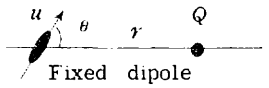	$-Qu\cos\theta/4\pi\varepsilon_0 r^2$
	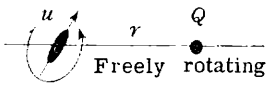	$-Q^2u^2/6(4\pi\varepsilon_0)^2kTr^4$
Dipole–dipole	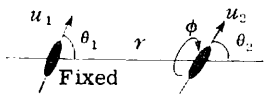	$-u_1u_2[2\cos\theta_1\cos\theta_2 - \sin\theta_1\sin\theta_2\cos\phi]/4\pi\varepsilon_0 r^3$
	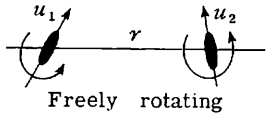	$-u_1^2u_2^2/3(4\pi\varepsilon_0)^2kTr^6$ (Keesom energy)
Charge–non-polar	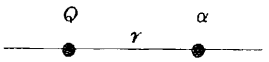	$-Q^2\alpha/2(4\pi\varepsilon_0)^2r^4$
Dipole–non-dipolar	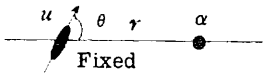	$-u^2\alpha(1+3\cos^2\theta)/2(4\pi\varepsilon_0)^2r^6$
	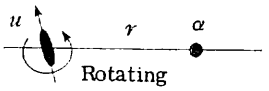	$-u^2\alpha/(4\pi\varepsilon_0)^2r^6$ (Debye energy)
Two non-polar molecules	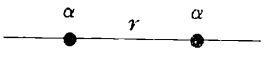	$-\frac{3}{4}\frac{h\nu\alpha^2}{(4\pi\varepsilon_0)^2r^6}$ (London dispersion energy)
Hydrogen bond	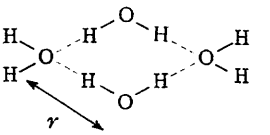	Complicated, short range, energy roughly proportional to $-1/r^2$

Fig. 2.2. Common types of interactions between atoms, ions and molecules in vacuum. $w(r)$ is the interaction free energy (in J); Q, electric charge (C); u, electric dipole moment (C m); α, electric polarizability ($C^2 m^2 J^{-1}$); r, distance between interacting atoms or molecules (m); k, Boltzmann constant (1.381×10^{-23} J K^{-1}); T, absolute temperature (K); h, Planck's constant (6.626×10^{-34} J s); ν, electronic absorption (ionization) frequency (s^{-1}); ε_0, dielectric permittivity of free space (8.854×10^{-12} $C^2 J^{-1} m^{-1}$). The force is obtained by differentiating the energy $w(r)$ with respect to distance r.

a solvent medium involve polarization effects. Third, there are forces that are *quantum mechanical* in nature. Such forces give rise to *covalent* or *chemical bonding* (including charge-transfer interactions) and to the repulsive *steric* or *exchange interactions* (due to the Pauli exclusion principle) that balance the attractive forces at very short distances.

These three categories should be considered as neither rigid nor exhaustive: for certain types of forces, e.g., van der Waals forces, an unambiguous classification is not possible, while some intermolecular interactions (e.g., magnetic forces) will not even be mentioned, since for the systems we shall consider, they are always very weak. A commonly encountered and even more artificial classification of forces into short-range forces and long-range forces will not be adhered to here except in an intuitive sense whereby short-range forces refer to those interactions occurring at or very near atomic or molecular contacts.

Falling into the above categories are a number of fairly distinct interactions whose pair potentials in vacuum are given in Fig. 2.2. In the following chapters these will be considered in turn, and in the process we shall introduce important conceptual aspects of intermolecular forces especially for interactions occurring in a medium: in a condensed medium, whether liquid or solid, the force between two molecules depends on whether they are immobilized or free to rotate (see Fig. 2.2) and is rarely given by simply dividing the vacuum interaction by the medium's dielectric constant, ε.

PROBLEMS AND DISCUSSION TOPICS

2.1 For molecules constrained to interact on a surface (as occurs on adsorption and in surface monolayers) there is a 'two-dimensional' van der Waals equation of state, analogous to the three-dimensional one (Eq. (2.21)). This may be written as

$$(\Pi + a/A^2)(A - b) = kT, \tag{2.29}$$

where Π is the externally applied surface pressure (in units of $\mathrm{N\,m^{-1}}$), A the mean area occupied per molecule, and a and b are constants. Derive this equation for molecules of diameter σ interacting with a van der Waals-type interaction pair potential given by $w(r) = -C/r^6$, and find the relation between the constants a, b and C, σ.

Can this approach, which predicts the existence of a gas–liquid transition, be extended to one-dimension? (*Hint*: carefully check the initial assumptions of this approach.)

2.2 Why do the attractive forces between the molecules of a gas affect the pressure of the gas while the attractive forces between the gas molecules and the wall molecules do not?

2.3 Why is there no simple rule, such as Trouton's Rule, relating the latent heat of melting to the melting temperature?

2.4 In Section 1.3 it is argued that long-range effects could arise for certain types of intermolecular potentials. Can you think of any examples (e.g., dipolar molecules, two-dimensional structures, metals, liquid crystals), explaining why and how the long-range effects manifest themselves. (Use Fig. 2.2 and other literature sources.)

CHAPTER 10

CONTRASTS BETWEEN INTERMOLECULAR, INTERPARTICLE AND INTERSURFACE FORCES

10.1 SHORT-RANGE AND LONG-RANGE EFFECTS OF A FORCE

We are told that when an apple fell on Newton's head it set in motion a thought process that eventually led Newton to formulate the law of gravity. The conceptual breakthrough in this discovery was the recognition that the force that causes apples to fall is the same force that holds the moon in a stable orbit around the earth.

On earth, gravity manifests itself in many different ways: in determining the height of the atmosphere; the capillary rise of liquids, and the behaviour of waves and ripples. In biology it decrees that animals that live in the sea (where the effect of gravity is almost negligible) can be larger than the largest possible land animal; that heavy land animals such as elephants must have short thick legs while a man or a spider can have proportionately long thin legs; that larger birds must have progressively larger wings (e.g., eagles and storks) while smaller birds, flies and bees can have relatively small light wings; that only small animals can carry many times their own weight (e.g., ants), and much else (Thompson, 1968). But beyond the immediate vicinity of the earth's surface and out to the outer reaches of space this same force now governs the orbits of planets, the shapes of nebulae and galaxies, the rate of expansion of the universe, and, ultimately, its age. The first group of phenomena—those occurring locally on the earth's surface—may be thought of as the *short-range* effects of the gravitational force, while the second and very different types of phenomena occurring on a cosmological scale may be thought of as the *long-range* effects of gravity.

Intermolecular forces are no less versatile in the way the same force can have very different effects at short and long range, though here 'short range' usually means at or very close to molecular contact (< 1 nm) while 'long-range' forces are rarely important beyond 100 nm (0.1 μm). In Part I we saw that the properties of gases and the cohesive strengths of condensed

phases are determined mainly by the interaction energies of molecules in contact $\omega(\sigma)$, i.e., molecules interacting with their immediate neighbours. For example, the van der Waals pair energy of two neighbouring molecules is at least 64 times stronger than that between next nearest neighbours ($1/\sigma^6$ compared to $1/(2\sigma)^6$). Only the Coulomb interaction is effectively long ranged in that the energy decays slowly, as $1/r$, and remains strong at large distances. However, in a medium of high dielectric constant such as water the strength of the Coulomb interaction is much reduced as is its range due to *electroneutrality* and *ionic screening* effects (Chapter 12).

We may therefore conclude that apart from ionic crystals (Chapter 3) the properties of solids and liquids are determined mainly by the molecular binding forces, i.e. by the strength of the interactions at or very near molecular contact, the long-range nature of the interaction (e.g., the exact distance dependence of the force law) playing only a minor role.

A very different situation arises when we consider the interactions of macroscopic particles or surfaces, for now when all the pair potentials between the molecules in each body is summed we shall find (i) that the net interaction energy is proportional to the size (e.g. radius) of the particles, so that the energy can be very much larger than kT even at separations of 100 nm or more, and (ii) that the energy and force decay much more slowly with the separation. All these characteristics make the interactions between macroscopic bodies effectively of much longer range than those between molecules even though the same basic type of force may be operating in each case.

Furthermore, if the force law is not monotonic (not purely attractive or repulsive) then all manner of behaviour may arise depending on the specific form of the long-range distance dependence of the interaction. This is illustrated in Fig. 10.1. For example, consider the purely attractive interaction of Fig. 10.1a. If both molecules and particles experience the same type of interaction, both will be attracted to each other, and the thermodynamic properties of an assembly of molecules in the gas or condensed phase will be determined by the depth of the potential well at contact, as will the adhesion energy of two particles. However, for the energy law in Fig. 10.1b two molecules will still attract each other since the energy barrier is negligibly small compared to kT, but two macroscopic particles will effectively repel each other since the energy barrier is now too high to surmount. Under such circumstances particles dissolved in a medium will remain dispersed even though the ultimate *thermodynamic equilibrium state* is the aggregated state.

We thus encounter another important difference between molecular and particle interactions, namely, that particles can be (and often are) trapped in some *kinetic* or *metastable state* if there is a sufficiently high energy barrier that prevents them from accessing all parts of their interaction potential over

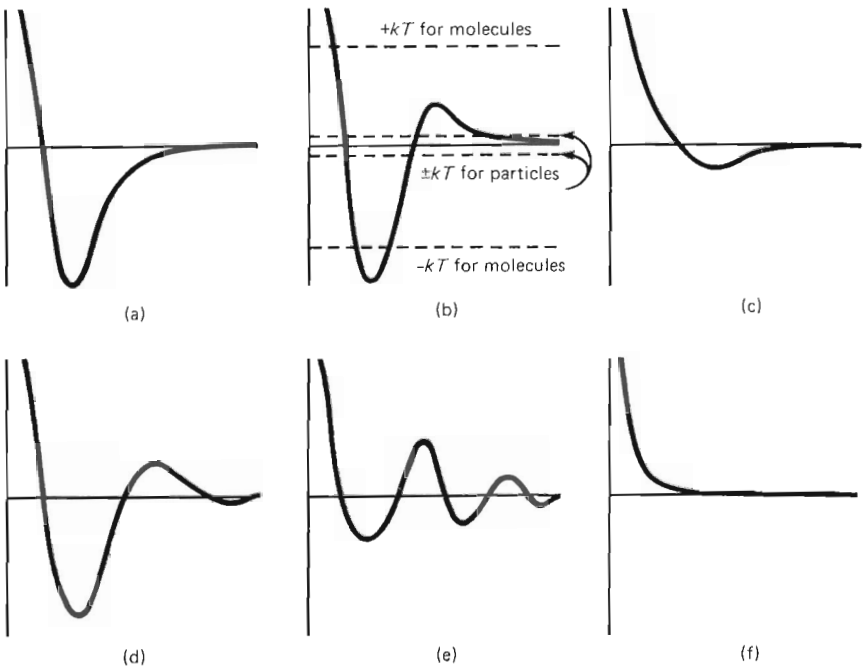

Fig. 10.1. Typical interaction potentials encountered between molecules and macroscopic particles in a medium. (a) This potential is typical of vacuum interactions but is also common in liquids. Both molecules and particles attract each other. (b) Molecules attract each other; particles effectively repel each other. (c) Weak minimum. Molecules repel, particles attract. (d) Molecules attract strongly, particles attract weakly. (e) Molecules attract weakly, particles attract strongly. (f) Molecules repel, particles repel.

some reasonable time period. Figure 10.1 illustrates some other types of commonly occurring intermolecular and intersurface potential functions and the different effects they can have on molecule–molecule and particle–particle interactions. In the following chapters we shall see how such interaction potentials actually arise in different systems.

□ ● **WORKED EXAMPLE** ●

Question: Consider a 10% by weight dispersion of glass particles of radius $a = 100$ nm in water at room temperature interacting via a potential as shown in Fig. 10.1b. Estimate what the energy barrier would have to be (in units of kT) for the particles to remain dispersed over a period of one day.

Answer: The mean Brownian velocity, v, per particle will be given by $\frac{1}{2}mv^2 \approx kT$, where $m = 1.3 \times 10^{-17}$ kg is the particle mass (assuming a density

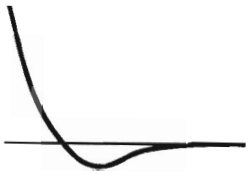

(c)

(f)

lecules and macroscopic
interactions but is also
ıer. (b) Molecules attract
ıimum. Molecules repel,
:t weakly. (e) Molecules
ticles repel.

some other types of
)tential functions and
and particle–particle
ıow such interaction

ss particles of radius
ı a potential as shown
have to be (in units
iod of one day.

:le will be given by
:s (assuming a density

of 3×10^3 kg m^{-3}). Thus we obtain $v = 0.025$ m s^{-1}. The number of particles per unit volume is 8×10^{18} m^{-3}, so that their mean separation is about 5×10^{-7} m (500 nm). Thus the time between collisions will be about $5 \times 10^{-7}/0.025 = 2 \times 10^{-5}$ s, so that the number of collisions per day will be $60 \times 60 \times 24/2 \times 10^{-5} \approx 4 \times 10^9$. We therefore require the condition that the probability of two colliding particles overcoming their energy barrier ΔW should be less than $1/(4 \times 10^9) = 2.5 \times 10^{-10}$. Putting $2.5 \times 10^{-10} = e^{-\Delta W/kT}$ we obtain $\Delta W/kT = 22$. Thus the energy barrier should be in excess of about $22kT$ to ensure kinetic stability, i.e. that most of the particles remain dispersed, over a 24 h period. (Note: a more rigorous calculation shows that the collision rate would be significantly lower due to viscous drag effects, and that an energy barrier of only 16 kT is needed to keep the system stable.) □

The interactions of 'soft' particles, e.g. those composed of flexible surfactant or polymer molecules, are particularly subtle due to the interplay of the short-range and long-range forces. The sizes and shapes of such 'self-assembling' molecular aggregates are regulated by the short-range interactions between the molecules, which are sensitive to electrolyte concentration, pH, temperature, etc. On the other hand, the long-range interactions between these aggregates—those that determine whether they will attract or repel each other—are also sensitve to these variables. Thus, different parts of the intermolecular interaction potential govern very different properties in these systems. The interdependence of short-range and long-range forces and, consequently, of *intraparticle* and *interparticle* forces is discussed in Part III.

10.2 INTERACTION POTENTIALS BETWEEN MACROSCOPIC BODIES

In this section we shall relate the pair interaction between two molecules to the interaction between a molecule and a flat surface, between two spherical particles (or two curved surfaces), between a spherical particle and a flat surface, and between two flat surfaces.

Molecule–surface interaction

Let us once again assume that the pair potential between two atoms or small molecules is purely attractive and of the form $w(r) = -C/r^n$. Then, with the further assumption of *additivity*, the net interaction energy of a molecule and the planar surface of a solid made up of like molecules (Fig. 10.2a) will be the sum of its interactions with all the molecules in the body. For molecules in a circular ring of cross-sectional area $dx\,dz$ and radius x, the ring volume

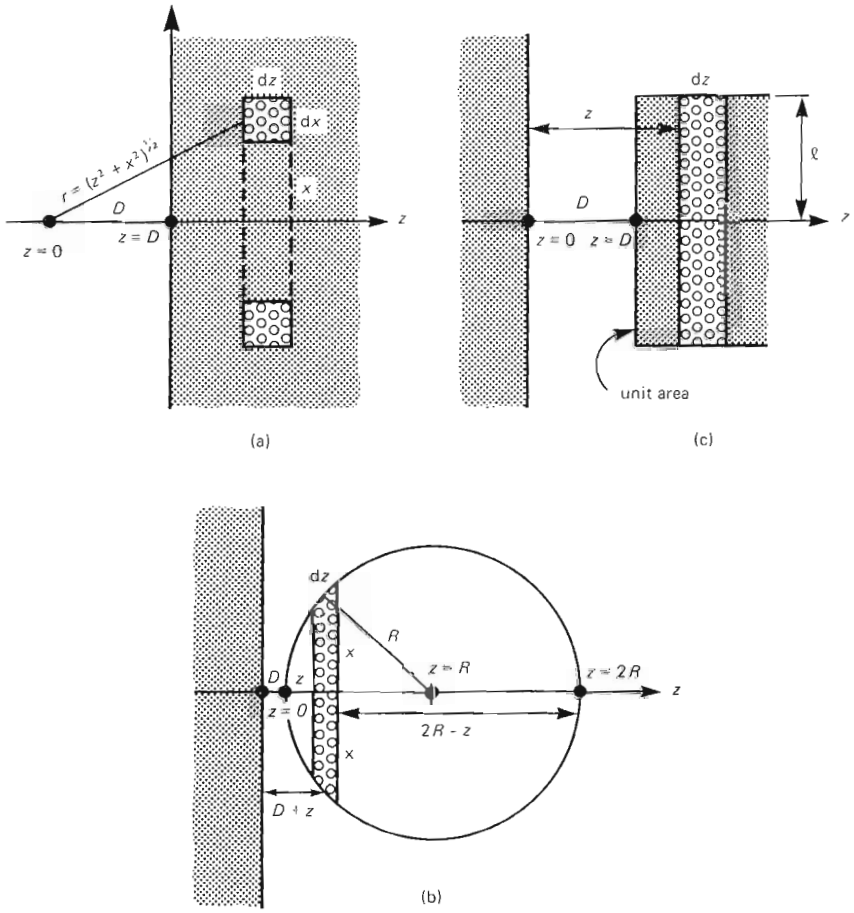

Fig. 10.2. Methods of summing (integrating) the interaction energies between molecules in condensed phases to obtain the interaction energies between macroscopic bodies. (a) Molecule near a flat surface or 'wall'. (b) Spherical particle near a wall ($R \gg D$). (c) Two planar surfaces ($l \gg D$).

is $2\pi x\,dx\,dz$, and the number of molecules in the ring will be $2\pi\rho x\,dx\,dz$, where ρ is the number density of molecules in the solid. The net interaction energy for a molecule at a distance D away from the surface will therefore be

$$w(D) = -2\pi C\rho \int_{z=-D}^{z=\infty} dz \int_{x=0}^{x=\infty} \frac{x\,dx}{(z^2 + x^2)^{n/2}} = \frac{2\pi C\rho}{(n-2)} \int_D^\infty \frac{dz}{z^{n-2}}$$

$$= -2\pi C\rho/(n-2)(n-3)D^{n-3} \qquad \text{for } n > 3, \tag{10.1}$$

which for $n = 6$ (van der Waals forces) becomes

$$w(D) = -\pi C\rho/6D^3. \tag{10.2}$$

The corresponding force, $F = \partial w(D)/\partial D = -\pi C\rho/2D^4$, could of course have been derived in a similar way by summing (integrating) all the pair forces resolved along the z axis.

Sphere–surface and sphere–sphere interaction

We can now calculate the interaction energy of a large sphere of radius R and a flat surface (Fig. 10.2b). First, from the chord theorem, Eq. (9.7), we know that for the circle: $x^2 = (2R - z)z$. The volume of a thin circular section of area πx^2 and thickness dz is therefore $\pi x^2\, dz = \pi(2R - z)z\, dz$, so that the number of molecules contained within this section is $\pi\rho(2R - z)z\, dz$, where ρ is the number density of molecules in the sphere. Since all these molecules are at a distance $(D + z)$ from the planar surface, the net interaction energy is, using Eq. (10.1),

$$W(D) = -\frac{2\pi^2 C\rho^2}{(n-2)(n-3)} \int_{z=0}^{z=2R} \frac{(2R - z)z\, dz}{(D+z)^{n-3}}. \tag{10.3}$$

For $D \ll R$, only small values of z ($z \approx D$) contribute to the integral, and we obtain[1]

$$W(D) = -\frac{2\pi^2 C\rho^2}{(n-2)(n-3)} \int_0^{\infty} \frac{2Rz\, dz}{(D+z)^{n-3}}$$

$$= -\frac{4\pi^2 C\rho^2 R}{(n-2)(n-3)(n-4)(n-5)D^{n-5}}, \tag{10.4}$$

which for $n = 6$ (van der Waals forces) becomes

$$W(D) = -\pi^2 C\rho^2 R/6D. \tag{10.5}$$

Note that the interaction energy is proportional to the radius of the sphere and that it decays as $1/D$, very much slower than the $1/r^6$ dependence of the intermolecular pair interaction.

[1] To avoid confusion we shall use W and D to denote the interaction free energies of macroscopic bodies whose surfaces are at a distance D apart, reserving w and r for the interactions of atoms and molecules.

For $D \gg R$, we may replace $(D + z)$ in the denominator of Eq. (10.3) by D, and we then obtain

$$W(D) = -\frac{2\pi^2 C\rho^2}{(n-2)(n-3)} \int_0^{2R} \frac{(2R - z)z \, dz}{D^{n-3}} = -\frac{2\pi C\rho(4\pi R^3\rho/3)}{(n-2)(n-3)D^{n-3}}. \tag{10.6}$$

Since $4\pi R^3\rho/3$ is simply the number of molecules in the sphere, the above is essentially the same as Eq. (10.1) for the interaction of a molecule (or small sphere) with a surface. It is left as an exercise for the interested reader to show that for two spheres of equal radii R whose surfaces are at a small distance D apart ($R \gg D$), their interaction energy is one half that given by Eq. (10.4) or (10.5), while for two spheres far apart ($D \gg R$) the energy varies as $-1/D^n$ as for two molecules. At intermediate separations ($R \approx D$) the expression for the interaction potential is more complicated but remains analytic (Hamaker, 1937).

Surface–surface interactions

Let us now calculate the interaction energy of two planar surfaces a distance D apart. For two infinite surfaces, the result will be infinity, and so we have to consider the energy per unit surface area. Let us start with a thin sheet of molecules of unit area and thickness dz at a distance z away from an extended surface of *larger* area (Fig. 10.2c). From Eq. (10.1) the interaction energy of this sheet with the surface is $-2\pi C\rho(\rho \, dz)/(n-2)(n-3)z^{n-3}$. Thus, for the two surfaces, we have

$$W(D) = -\frac{2\pi C\rho^2}{(n-2)(n-3)} \int_D^{\infty} \frac{dz}{z^{n-3}} = -\frac{2\pi C\rho^2}{(n-2)(n-3)(n-4)D^{n-4}}, \tag{10.7}$$

which for $n = 6$ becomes

$$W(D) = -\pi C\rho^2/12D^2 \qquad \text{per unit area.} \tag{10.8}$$

It is important to note that Eqs (10.7) and (10.8) are for unit area of one surface interacting with an infinite area of another surface. In practice this usually amounts to two unit areas of both surfaces, but it is strictly applicable only when D is small compared to the lateral dimensions of the surfaces.

10.3 EFFECTIVE INTERACTION AREA OF TWO SPHERES: THE LANGBEIN APPROXIMATION

When two large spheres or a sphere and a flat surface are close together, one sometimes wants to know what is their 'effective area' of interaction. First, we may note that no matter how large a sphere becomes it *never* approaches the behaviour of a flat surface. Its interaction energy will increase linearly with radius R (Eq. (10.4)), but the distance dependence of the interaction will not change to that corresponding to two planar surfaces. However, the concept of an effective 'interaction zone' and effective 'interaction area', A_{eff}, are useful. If we compare Eq. (10.4) for a sphere near a surface with Eq. (10.7) for two surfaces, we find that the interaction of a sphere and a surface is the same as that of two planar surfaces *at the same surface separation* D if their area is

$$A_{\text{eff}} = 2\pi RD/(n-5)$$
$$= 2\pi RD \qquad \text{for } n = 6. \tag{10.9}$$

From Fig. 10.2b and Eq. (9.7) this area is simply equal to πx^2 when $z = D$ (so long as $R \gg D$). In other words, the effective area of interaction of a sphere with a surface is the circular zone centred at a distance $-D$ from the surface (inside the sphere). This is known as the *Langbein approximation.*

The effective area of interaction increases linearly with both R and D as may be expected. For example, for a sphere of radius $R = 1\ \mu$m at a distance $D = 1$ nm from a wall, the effective interaction area is about $2\pi RD \approx 10^{-14}\ \text{m}^2$ or 10 000 nm^2, which corresponds to an area of radius $\sim$45 nm. At contact, when $D \approx 0.3$ nm, this radius falls to 25 nm, though in practice elastic flattening generally significantly increases the contact area (see Section 15.5).

10.4 INTERACTIONS OF LARGE BODIES COMPARED TO THOSE BETWEEN MOLECULES

The geometries analysed above are the most commonly encountered. In the next chapter we shall look specifically at the van der Waals interactions of these and of other geometries as well (e.g., cylinders). Meanwhile, let us consider some of the implications of the interaction potentials obtained so far.

First we may note that for two macroscopic bodies, the interaction energy generally decays much more slowly with distance than it does for two molecules. For example, whereas the van der Waals energy between atoms

and molecules is of short range, having an inverse sixth-power distance dependence, the van der Waals energy between large condensed bodies decays more slowly with distance (cf. $1/D$ for spheres, $1/D^2$ for planar surfaces) and is effectively of much longer range. This is yet another manifestation of the long-range nature of interparticle forces.

Second, the van der Waals interaction energy of a small molecule of diameter σ with a wall is given by Eq. (10.2) as $w(D) = -\pi C\rho/6D^3$. At contact we may put $D \approx \sigma$ and $\rho \approx \sqrt{2}/\sigma^3$ (corresponding to a close packed solid) and obtain

$$w(\sigma) \approx -\sqrt{2}\pi C/6\sigma^6 \approx -0.74C/\sigma^6 \tag{10.10}$$

which is of the same order as $-C/\sigma^6$ for two small molecules in contact. Likewise, for a sphere of atomic dimensions ($R = \sigma/2$) in contact with a wall ($D = \sigma$), we find from Eq. (10.5) that

$$W(\sigma) \approx -2\pi^2 C/12\sigma^6 \approx -1.6C/\sigma^6, \tag{10.11}$$

while for two spheres

$$W(\sigma) \approx -0.8C/\sigma^6, \tag{10.12}$$

which again are very close to the molecule–molecule pair potential at contact. However, once the size of a sphere increases above atomic dimensions (i.e., once $R > \sigma$), then at contact ($D = \sigma$) Eq. (10.5) becomes

$$W(\sigma) \approx -2\pi^2 CR/6\sigma^7 \approx -1.6(2R/\sigma)C/\sigma^6,$$

which reduces to Eq. (10.11) only for small radii, of order $R \approx \sigma/2 \approx 0.1$–$0.2$ nm, but which increases linearly with R for larger spheres. Likewise for the interaction of two spheres. This is an important result. It shows that for diameters $2R$ beyond about 0.5 nm, a molecule must already be considered as a (small) particle or else the strength of its interaction will be underestimated. The higher strength of the measured interaction between large molecules over that predicted on the assumption that $D = 2R$ was seen in Table 6.1 for CCl_4 but not for the smaller molecules. In conclusion, while for two atoms or small molecules the contact interaction energy has no explicit size dependence, that between larger particles increases linearly with their radius.

As regards the stabilizing repulsive forces between large bodies, these too manifest themselves in quite different ways when acting between macroscopic bodies. While the short-range steric or Born repulsion between individual

molecules may remain the same (see Problem 10.5), large spheres will deform elastically or even plastically when in contact under a large adhesive force. The stabilizing repulsive forces of macroscopic particles therefore also involve the elastic properties of the materials (discussed further in Chapters 15 and 18).

10.5 INTERACTION ENERGIES AND INTERACTION FORCES: THE DERJAGUIN APPROXIMATION

So far we have been dealing mainly with interaction *energies* rather than the *forces* experienced by molecules and particles. This is because most experimental data on molecular interactions are of a thermodynamic nature and therefore more readily understood in terms of interaction energies, as we saw in Part I. However, between macroscopic bodies it is the forces between them that are often easier to measure, and of greater interest, than their interaction energies.

It is therefore desirable to be able to relate the force law $F(D)$ between two curved surfaces to the interaction free energy $W(D)$ between two planar surfaces. Luckily, a simple relation exists for the two geometries most commonly encountered, viz. two flat surfaces and two spheres (a sphere near a flat surface being a special case of two spheres with one sphere very much larger than the other). A glance at Eq. (10.4) shows that for the additive intermolecular pair potential $w(r) = -C/r^n$, the value of $F(D)$ for a sphere near a flat surface is

$$F(D) = -\frac{\partial W(D)}{\partial D} = -\frac{4\pi^2 C\rho^2 R}{(n-2)(n-3)(n-4)D^{n-4}}. \tag{10.13}$$

This force law can be seen to be simply related to $W(D)$ per unit area of two planar surfaces, Eq. (10.7), by

$$F(D)_{\text{sphere}} = 2\pi R W(D)_{\text{planes}}. \tag{10.14}$$

This is a very useful relationship, and while it was derived for the special case of an additive inverse power potential, it is in fact valid for any type of force law, as will now be shown.

Assume that we have two large spheres of radii R_1 and R_2 a small distance D apart (Fig. 10.3). If $R_1 \gg D$ and $R_2 \gg D$, then the force between the two spheres can be obtained by integrating the force between small circular regions of area $2\pi x\,dx$ on one surface and the opposite surface, which is assumed to be locally flat and at a distance $Z = D + z_1 + z_2$ away. The net

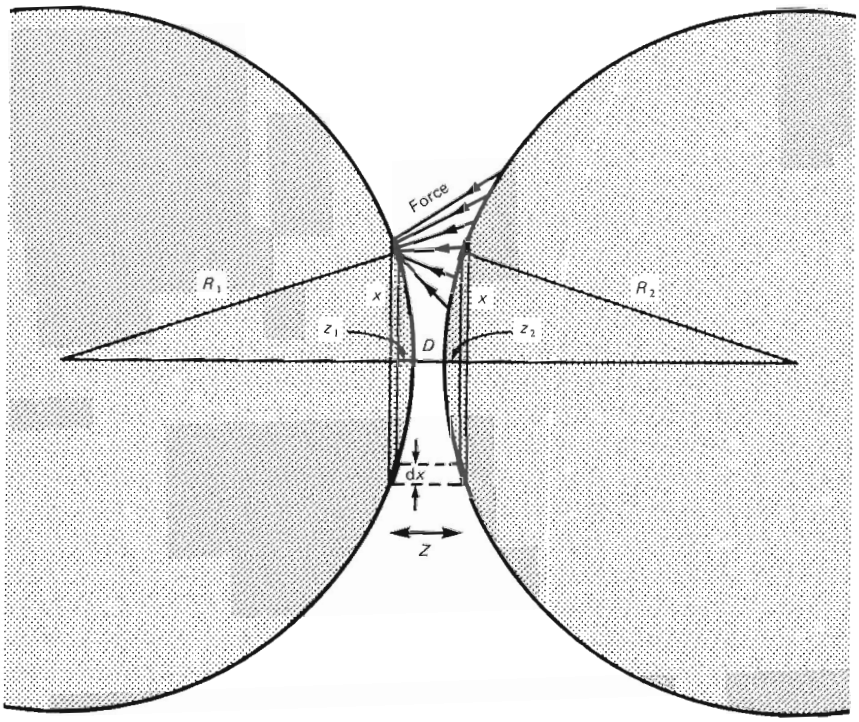

Fig. 10.3. The Derjaguin approximation (Derjaguin, 1934), which relates the force law $F(D)$ between two spheres to the energy per unit area $W(D)$ of two flat surfaces by $F(D) = 2\pi[R_1R_2/(R_1 + R_2)]W(D)$.

force between the two spheres (in the z direction) is therefore

$$F(D) = \int_{Z=D}^{Z=\infty} 2\pi x \, \mathrm{d}x f(Z), \tag{10.15}$$

where $f(Z)$ is the normal force per unit area between two flat surfaces. Since from the Chord Theorem $x^2 \approx 2R_1z_1 = 2R_2z_2$, we have

$$Z = D + z_1 + z_2 = D + \frac{x^2}{2}\left(\frac{1}{R_1} + \frac{1}{R_2}\right) \tag{10.16}$$

and

$$\mathrm{d}Z = \left(\frac{1}{R_1} + \frac{1}{R_2}\right) x \, \mathrm{d}x, \tag{10.17}$$

so that Eq. (10.15) becomes

$$F(D) \approx \int_D^\infty 2\pi\left(\frac{R_1 R_2}{R_1 + R_2}\right) f(Z)\,\mathrm{d}Z = 2\pi\left(\frac{R_1 R_2}{R_1 + R_2}\right) W(D), \qquad (10.18)$$

which gives the force between two spheres in terms of the energy per unit area of two flat surfaces at the same separation D. Equation (10.18) is known as the *Derjaguin approximation* (Derjaguin, 1934). It is applicable to any type of force law, whether attractive, repulsive or oscillatory, so long as the range of the interaction and the separation D is much less than the radii of the spheres. It is a useful theoretical tool, since it is usually easiest to derive the interaction energy for two planar surfaces (rather than for curved surfaces). It is also useful for interpreting experimental data and it has been well verified experimentally, as discussed in Chapters 11–15.

From the Derjaguin approximation, Eq. (10.18), we may deduce the following:

(i) If one sphere is very large so that $R_2 \gg R_1$, we obtain $F(D) = 2\pi R_1 W(D)$, which is the same as Eq. (10.14) and corresponds to the limiting case of a sphere near a flat surface.

(ii) For two equal spheres of radii $R = R_1 = R_2$, we obtain $F(D) = \pi R W(D)$, which is half the value for a sphere near a flat surface.

(iii) For two spheres in contact ($D = \sigma$), the value of $W(\sigma)$ can be associated with 2γ, where γ is the conventional surface energy per unit area of a surface. Eq. (10.18) then becomes

$$F(\sigma) = F_{\mathrm{ad}} = \frac{4\pi\gamma R_1 R_2}{(R_1 + R_2)} \qquad (10.19)$$

which gives the adhesion force F_{ad} between two spheres in terms of their surface energy. Adhesion forces are discussed in Chapter 15.

(iv) Perhaps the most intriguing aspect of the Derjaguin approximation is that it tells us that the distance dependence of the force between two curved surfaces can be quite different from that between two flat surfaces even though the same type of force is operating in both. This is illustrated in Fig. 10.4, where we see that a purely repulsive force between two curved surfaces can be attractive between two planar surfaces (over a certain distance regime), with equilibrium at some finite separation (Fig. 10.4b). Conversely, a purely attractive force between curved surfaces can become repulsive between two planar surfaces (Fig. 10.4c).

(v) Finally, it may be readily shown that for two cylinders of radii R_1 and

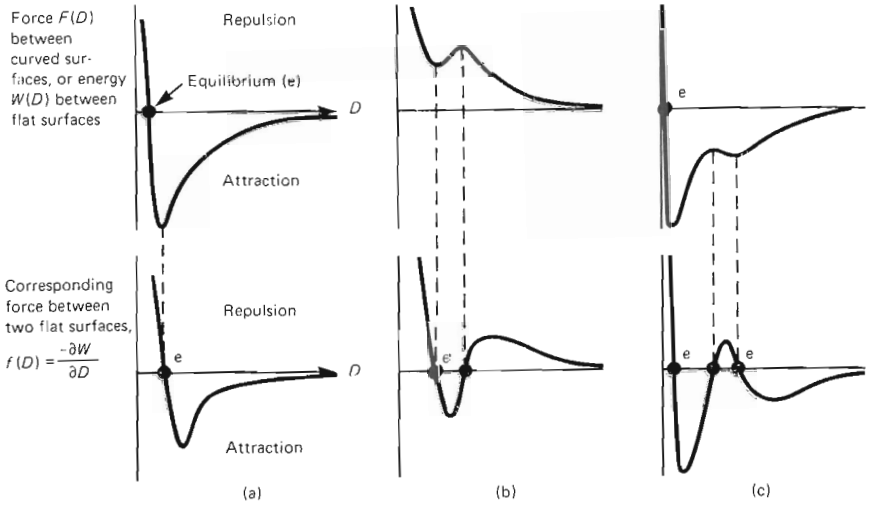

Fig. 10.4. Top row: force laws between two curved surfaces (e.g., two spherical particles). Bottom row: corresponding force laws between two flat surfaces. Note that stable equilibrium occurs only at points marked e where the force is zero ($f = 0$) *and* the force curve has negative slope; the other points where $f = 0$ are unstable.

R_2 crossed at an angle θ to each other, the Derjaguin approximation becomes

$$F(D) = 2\pi\sqrt{R_1 R_2}\,W(D)/\sin\theta, \qquad \text{for } D \ll R_1, R_2. \tag{10.20}$$

Note that for two cylinders of equal radii $R = R_1 = R_2$, crossed at right angles to each other ($\theta = 90°$, $\sin\theta = 1$) the above reduces to the same result as for a sphere of radius R near a flat surface. In other words the interaction of two orthogonal cylinders is the same as that of a sphere and a wall if all three radii are the same.

□ ● **WORKED EXAMPLE** ●

Question: Two orthogonal cylinders of equal radius R are separated by a small distance D ($D \ll R$). Using purely geometrical arguments, show that the surface geometry around the contact region is the same, to first order, as for a sphere of the same radius R at the same distance D from a flat surface.

Answer: Referring to Fig. 10.5a, and using Eq. (9.7), we have $x^2 = 2RD_1$ and $y^2 = 2RD_2$. Referring to Fig. 10.5b, this implies $2R(D_1 + D_2) = x^2 + y^2 = r^2$. Thus $D_1 + D_2$ is constant if r is constant, i.e. if P describes a circle. Since the above equation is indistinguishable from that for a sphere of the same radius

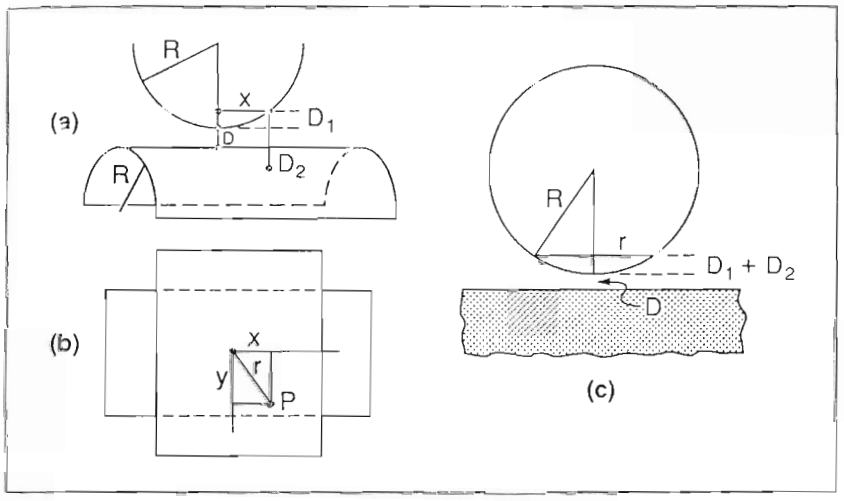

Fig. 10.5. Geometry of two crossed cylinders.

near a flat surface, Fig. 10.5c, we have proved that as far as interactions (and many other properties) are concerned the two geometries are locally equivalent. □

10.6 EXPERIMENTAL MEASUREMENTS OF INTERMOLECULAR AND SURFACE FORCES

When we come to consider experimental measurements of intermolecular forces we are confronted with a bewildering variety of data to draw upon. This is because almost any measurement in the below-10 eV category, whether in physics, chemistry or biology, is in some respect a measurement of intermolecular forces. For example, we have already seen how such a common property as the boiling point of a substance provides information on the strength of intermolecular binding energies. It is therefore difficult to make a list of experimental measurements of intermolecular forces; it is far better to draw upon whatever relevant data exist as the situation arises. This was done in Part I, and we shall continue with this practice in Parts II and III. However, different types of measurements do provide different insights and information, and in the rest of this chapter we shall categorize experiments according to the type of information they provide on intermolecular and intersurface interactions. First, let us recapitulate some of those already mentioned.

(i) Thermodynamic data on gases, liquids and solids (e.g., PVT data, boiling points, latent heats of vaporization, lattice energies) provide

information on the short-range attractive potentials between molecules. Adsorption isotherms provide information on the interactions of molecules with surfaces.

(ii) Physical data on gases, liquids and solids (e.g., molecular beam scattering experiments, viscosity, diffusion, compressibility, NMR, x-ray and neutron scattering of liquids and solids) provide information on the short-range interactions of molecules, especially their repulsive forces which give insight into molecular size and shape, and their involvement in the structure of condensed phases.

(iii) Thermodynamic data on liquids and liquid mixtures (e.g., phase diagrams, solubility, partitioning, miscibility, osmotic pressure) provide information on short-range solute–solvent and solute–solute interactions.

Such experimental data as listed in (i)–(iii) above often provide thermodynamic information only, so that direct access to the intermolecular potential functions (i.e., their distance dependence) is not possible. Thus, experimental PVT data may be compared with the van der Waals equation of state (Chapter 6), which contains terms to account for both the attractive and repulsive forces, but it does not give any information on the nature and range of the force laws themselves. To gain this information, some more direct measurement of forces is required. Of the various methods that have been devised for measuring molecular forces, the most direct employ macroscopic bodies or extended surfaces, where distances can be measured to within 0.1 nm, where the forces are large and measurable, and where entropic (thermal) effects are negligible. It is from such experiments (illustrated in Fig. 10.6) that many hard data on intermolecular and surface interactions have emerged.

(iv) Particle detachment and peeling experiments (Fig. 10.6a, b) provide information on particle adhesion forces and the adhesion energies of solid surfaces in contact (i.e., attractive short-range forces). Such experiments are important in powder technology, xerography, ceramic processing, the making of adhesive films and in understanding how cracks propagate in solids.

(v) Measuring the force between two macroscopic surfaces as a function of surface separation can provide the full force law of an interaction (Fig. 10.6c). Such direct force measurements are described in the next section.

(vi) Various surface studies such as surface tension and contact angle measurements give information on liquid–liquid and solid–liquid adhesion energies (Fig. 10.6d). When contact angles are measured under different atmospheric environments or as a function of time, these relatively simple experiments can provide surprisingly valuable insights into the states of surfaces and adsorbed films, and of molecular reorientation times at interfaces.

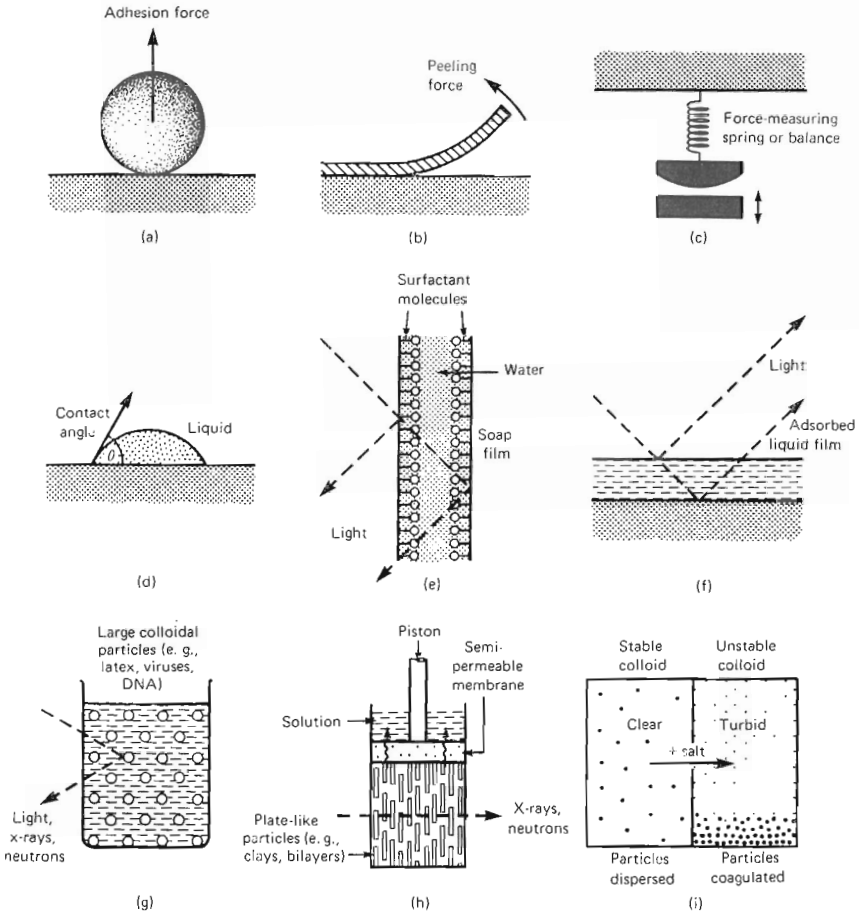

Fig. 10.6. Different types of measurements that provide information on the forces between particles and surfaces. (a) Adhesion measurements (practical applications: xerography, particle adhesion, powder technology, ceramic processing). (b) Peeling measurements (practical applications: adhesive tapes, material fracture and crack propagation). (c) Direct measurements of force as a function of surface separation (practical applications: testing theories of intermolecular forces). (d) Contact angle measurements (practical applications: testing wettability and stability of surface films, detergency). (e) Equilibrium thickness of thin free films (practical applications: soap films, foams). (f) Equilibrium thickness of thin adsorbed films (practical applications: wetting of hydrophilic surfaces by water, adsorption of molecules from vapour, protective surface coatings and lubricant layers, photographic films). (g) Interparticle spacing in liquids (practical applications: colloidal suspensions, paints, pharmaceutical dispersions). (h) Sheet-like particle spacings in liquids (practical applications: clay and soil swelling behaviour, microstructure of soaps and biological membranes). (i) Coagulation studies (practical application: basic experimental technique for testing the stability of colloidal preparations).

(vii) The thicknesses of free soap films and liquid films adsorbed on surfaces (Fig. 10.6e, f) can be measured as a function of salt concentration or vapour pressure. Such experiments provide information on the long-range repulsive forces stabilizing thick wetting films. Various optical techniques (e.g., reflected intensity, total internal reflection spectroscopy, or ellipsometry) have been used to measure film thickness to within 0.1 nm.

(viii) Dynamic interparticle separations and motions in liquids can be measured using NMR, light scattering, x-ray scattering and neutron scattering (Fig. 10.5g, h). In such experiments the particles can be globular or spherical (e.g., micelles, vesicles, colloidal particles, latex particles, viruses), sheet-like, (e.g., clays, lipid bilayers), or rod-like (e.g., DNA). The interparticle forces can be varied by changing the solution conditions, and their mean separation can be varied by changing the quantity of solvent, for example, by changing the hydrostatic or osmotic pressure via a semipermeable membrane. Notable among these techniques is the *Compression Cell* or *Osmotic Pressure Technique* (Homola and Robertson, 1976; LeNeveu *et al.*, 1976) from which the interaction force between particles can be obtained from the deviations from ideality in the PVT data. Such techniques are usually limited to measuring only the repulsive parts of a force law.

(ix) In coagulation studies on colloidal dispersions (Fig. 10.5i) the salt concentration, pH, or temperature of the suspending liquid medium (usually water) is changed until the dispersion becomes unstable and the particles coalesce (*coagulate* or *flocculate*). Coagulation rates can be very fast or very slow (see Worked Example in Section 10.1). Such studies provide information on the interplay of repulsive and attractive forces between particles in pure liquids as well as in surfactant and polymer solutions.

10.7 DIRECT MEASUREMENTS OF SURFACE AND INTERMOLECULAR FORCES

Most of the methods shown in Fig. 10.6 do not give the force law (the force as a function of distance) but rather the adhesion force or minimum energy at some particular state, e.g., the equilibrium state, of the system. Other methods, such as osmotic pressure measurements, involve the collective interactions of many molecules or particles so that the data gained tends to be of a thermodynamic nature and not directly translatable into a force law. The most unambiguous way to measure a force-law is to position two bodies close together and directly measure the force between them, e.g., from the deflection of a spring—very much as one would measure the force between two magnets. While the principle of direct force measurements is usually very straightforward, the challenge comes in measuring very weak forces at very small intermolecular or surface separations which must be controlled and measured to within 0.1 nm.

The first direct measurements of intermolecular forces were those of Derjaguin and coworkers (Derjaguin and Abrikossova, 1954; Derjaguin *et al.*, 1956) who measured the attractive van der Waals forces between a convex lens and a flat glass surface in vacuum. An electrobalance was used to measure the forces and an optical technique to measure the distance between two glass surfaces. Measurements were made in the distance regime 100–1000 nm, and the results fell within 50% of the predictions of the Lifshitz theory of van der Waals forces (Chapter 11).

These experiments opened the way for the slow but steady progress that has led to the highly sophisticated and versatile techniques that are used today for measuring the interactions between surfaces in vapours or liquids at the ångstrom resolution level. Both static (i.e. equilibrium) and dynamic (e.g. viscous) forces can now be studied with unprecedented precision providing information not only on the fundamental interactions in liquids but also into the structure of liquids adjacent to surfaces and other interfacial phenomena. Three techniques which can directly measure the force laws between two bodies of *macroscopic*, *colloidal* and *atomic* dimensions, respectively, will now be briefly described.

Measuring surface forces: the Surfaces Forces Apparatus (SFA)

During the last 20 years various direct force-measuring techniques have been developed which allow for the full force laws to be measured between two surfaces at the ångstrom resolution level (Israelachvili, 1989). Tabor and Winterton (1969) and Israelachvili and Tabor (1972, 1973) developed apparatuses for measuring the van der Waals forces between molecularly smooth mica surfaces in air or vacuum. The results using these new techniques confirmed the predictions of the Lifshitz theory of van der Waals forces (Chapter 11) down to surface separations as small as 1.5 nm. These techniques were then further developed for making measurements in liquids, which opened up a whole world of new phenomena of relevance to a much wider spectrum of surface science. We shall now describe one such apparatus which has become a standard research tool in many laboratories.

Figure 10.7 shows an SFA with which the force between two surfaces in controlled vapours or immersed in liquids can be directly measured (Israelachvili and Adams, 1978; Israelachvili, 1987b). The distance resolution is about 0.1 nm and the force sensitivity is about 10^{-8} N (10^{-6} g). Modified versions have been developed by Klein (1980), Parker *et al.* (1989a), Israelachvili and McGuiggan (1990), and Tonck *et al.* (1988) have extended the SFA method to opaque materials, replacing the optical technique for measuring distances (see below) by a capacitance method—the overall accuracy remaining about the same.

The SFA contains two curved molecularly smooth surfaces of mica

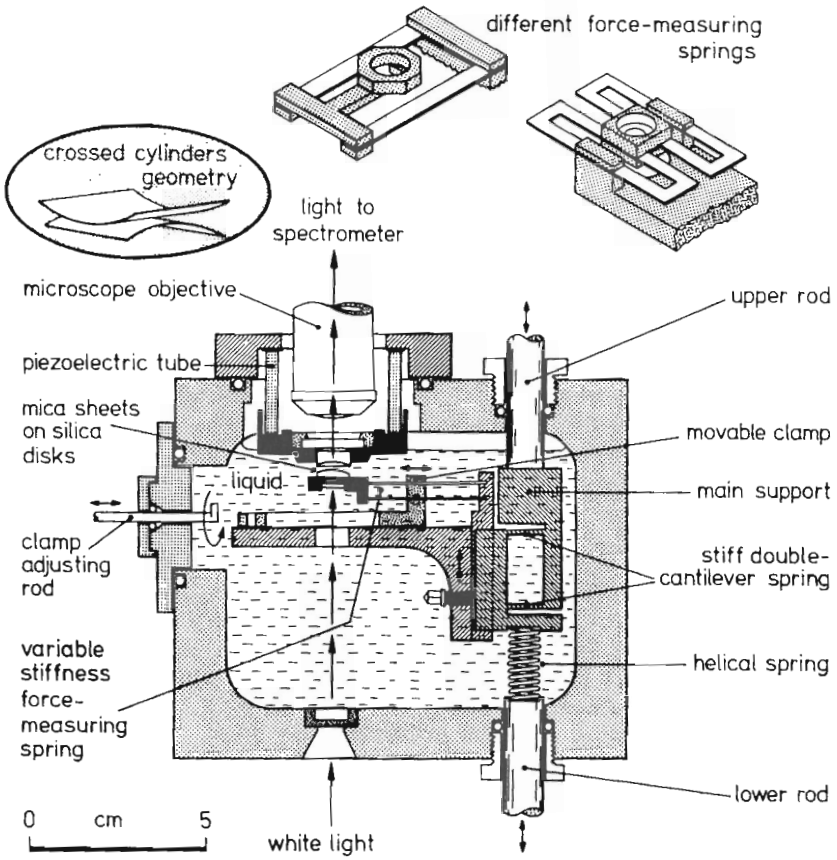

Fig. 10.7. Surface Forces Apparatus (SFA) for directly measuring the force laws between surfaces in liquids or vapours at the ångstrom resolution level. With the SFA technique two atomically smooth surfaces immersed in a liquid can be brought towards each other in a highly controlled way (the surface separation being controlled to 1 Å). As the surfaces approach each other they trap a very thin film of liquid between them and the forces between the two surfaces (across the liquid film) can be measured. In addition, the surfaces can be moved laterally past each other and the shear forces also measured during sliding. The results on many different liquids have revealed ultrathin film properties that are profoundly different from those of the bulk liquids, for example, that liquids can support both normal loads and shear stresses, and that molecular relaxations can take 10^{10} times longer in a 10 Å film that in the bulk liquid. Only molecular theories, rather than continuum theories, can explain such phenomena. However, most long-range interactions are adequately explained by continuum theories.

(of radius $R \approx 1$ cm) between which the interaction forces are measured using a variety of (interchangeable) force-measuring springs. The two surfaces are in a crossed cylinder configuration which is locally equivalent to a sphere near a flat surface or to two spheres close together (see Section 10.5).

-measuring springs

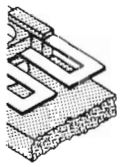

upper rod

movable clamp

main support

stiff double-cantilever spring

helical spring

lower rod

The separation between the two surfaces from microns down to molecular contact can be measured by use of an optical technique using multiple beam interference fringes called Fringes of Equal Chromatic Order (FECO). Here the two transparent mica sheets (each about 2 μm thick) are first coated with a semireflecting 50–60 nm layer of pure silver before they are glued onto the curved silica discs (silvered sides down). Once in position in the apparatus, as shown in Fig. 10.7, white light is passed vertically up through the two surfaces and the emerging beam is then focused onto the slit of a grating spectrometer. From the positions and shapes of the coloured FECO fringes seen in the spectrogram the distance between the two surfaces can be measured, usually to better than 0.1 nm, as can the exact shapes of the two surfaces and the refractive index of the liquid (or material) between them; the latter allows for reasonably accurate determinations of the quantity of material (e.g., lipid or polymer) deposited or adsorbed on the surfaces.

The distance between the two surfaces is controlled by use of a three-stage mechanism of increasing sensitivity: the coarse control (upper rod) allows positioning to within about 1 μm, the medium control (lower rod, which depresses the helical spring and which in turn bends the much stiffer double-cantilever spring by 1/1000 of this amount) allows positioning to about 1 nm. Finally, a piezoelectric crystal tube—which expands or contracts vertically by about 1 nm per volt applied axially across its cylindrical wall—is used for positioning to 0.1 nm.

Given the facility for moving the surfaces towards or away from each other and, independently, for measuring their separation (each with a sensitivity or resolution of about 0.1 nm), the force measurements themselves now become straightforward. The force is measured by expanding or contracting the piezoelectric crystal by a known amount and then measuring optically how much the two surfaces have actually moved; any difference in the two values when multiplied by the stiffness of the force-measuring spring gives the force difference between the initial and final positions. In this way, both repulsive and attractive forces can be measured and a full force law can be obtained over any distance regime. The force-measuring spring can be either a single-cantilever or a double-cantilever fixed-stiffness spring, or—as shown in Fig. 10.7—the spring stiffness can be varied during an experiment (by a factor of 1000) by shifting the position of the dove-tailed clamp using the adjusting rod. Other spring attachments, two of which are shown at the top of the figure, can also be used. Each of these springs are interchangeable and can be attached to the main support allowing for greater versatility in measuring strong or weak, attractive or repulsive forces.

Once the force F as a function of distance D is known for the two surfaces (of radius R), the force between any other curved surfaces simply scales by R (see Section 10.5). Furthermore, the adhesion or interfacial energy E per unit area between two *flat* surfaces is simply related to F by the Derjaguin

force laws between
the SFA technique
towards each other
Å). As the surfaces
em and the forces
ldition, the surfaces
ured during sliding.
roperties that are
liquids can support
an take 10^{10} times
ier than continuum
e interactions are

measured using
two surfaces are
lent to a sphere
tion 10.5).

approximation: $E = F/2\pi R$. Thus, for $R \approx 1$ cm, and given the measuring sensitivity in F of about 10^{-8} N, the sensitivity in measuring adhesion and interfacial energies is therefore about 10^{-3} mJ m^{-2} (erg cm^{-2}).

Over the past few years the SFA has identified and quantified most of the fundamental interactions occurring between surfaces in both aqueous solutions and nonaqueous liquids. These include the attractive van der Waals and repulsive electrostatic 'double-layer' forces, oscillatory (solvation or structural) forces, repulsive hydration forces, attractive hydrophobic forces, steric interactions involving polymeric systems, and capillary and adhesion forces. These forces are described in the following chapters.

Apart from testing theories of intermolecular forces, direct force measurements have also been useful in explaining or helping to understand more complex phenomena such as the second virial coefficients of colloidal dispersions (Gee *et al.*, 1990), the origin of the lower consulate points in the phase diagrams of certain surfactant–water mixtures (Claesson *et al.*, 1986b), the unexpected stability of certain colloidal dispersions in high salt (see Chapter 13), the crucial role of hydration and ion-correlation forces in clay swelling and ceramic processing (Quirk, 1968; Pashley and Quirk, 1984; Kjellander *et al.*, 1988; Velamakanni *et al.*, 1990; Horn, 1990), and the deformed shapes of adhering particles and vesicles (Bailey *et al.*, 1990).

Though mica, because of its molecularly smooth surface and ease of handling, is the primary surface used in SFA studies, there is currently much interest in developing alternative surfaces with different chemical and physical properties. Thus, the mica surface can be used as a substrate for adsorbing or depositing a thin film of some other material, for example, lipid monolayers or bilayers (see Chapter 18), metal films (Smith *et al.*, 1988; Parker and Christenson, 1988), polymer films (see Chapter 15), or other macromolecules such as proteins (Lee and Belfort, 1989). Alternative materials to mica sheets are also being developed. Thus Horn *et al.* (1988a, 1989a) have shown how molecularly smooth sapphire and silica sheets can be used in such studies, and Hirz *et al.* (1991) have studied carbon and metal oxide surfaces, sputtered as thin layers onto mica sheets which now act as substrate supports for these materials.

The scope of phenomena that can be studied using the SFA technique has recently been extended to measurements of dynamic interactions and time-dependent effects, for example, the viscosity of liquids in very thin films (Chan and Horn, 1985; Israelachvili, 1986, 1989), shear and frictional forces (Israelachvili *et al.*, 1988), and the fusion of lipid bilayers (Helm *et al.*, 1989).

Measuring colloidal forces: Total Internal Reflection Microscopy (TIRM)

The forces between two colloidal particles in a liquid can be weaker than 10^{-13} g (10^{-15} N) and yet still be important in determining the properties

CHAPTER 11

VAN DER WAALS FORCES BETWEEN SURFACES

11.1 THE FORCE LAWS FOR BODIES OF DIFFERENT GEOMETRIES: THE HAMAKER CONSTANT

As we saw in Part I, van der Waals forces play a central role in all phenomena involving intermolecular forces, for while they are not as strong as Coulombic or H-bonding interactions, they are always present. When we come to consider the long-range interactions between macroscopic particles and surfaces in liquids we shall find that the three most important forces are the van der Waals, electrostatic and steric-polymer forces, and that at shorter distances (below 1 to 3 nm) solvation and other types of steric forces often dominate over both.

Let us begin by deriving the van der Waals interaction energies in vacuum for pairs of bodies of different geometries. Starting at the simplest level we shall assume that the interaction is *non-retarded* and *additive*. In Chapter 10 we saw that for an interatomic van der Waals pair potential of the form $w(r) = -C/r^6$, one may sum (integrate) the energies of all the atoms in one body with all the atoms in the other and thus obtain the 'two-body' potential for an atom near a surface (Eq. (10.2)), for a sphere near a surface (Eq. (10.5)), or for two flat surfaces (Eq. (10.8)). This procedure can be carried out for other geometries as well. The resulting interaction laws for some common geometries are shown in Fig. 11.1, given in terms of the conventional Hamaker constant

$$A = \pi^2 C \rho_1 \rho_2 \tag{11.1}$$

after Hamaker (1937), who together with Bradley (1932), Derjaguin (1934), and de Boer (1936), did much of the earlier work that advanced understanding of the forces between macroscopic bodies.

Typical values for the Hamaker constants of condensed phases, whether solid or liquid, are about 10^{-19} J for interactions across *vacuum*. For example,

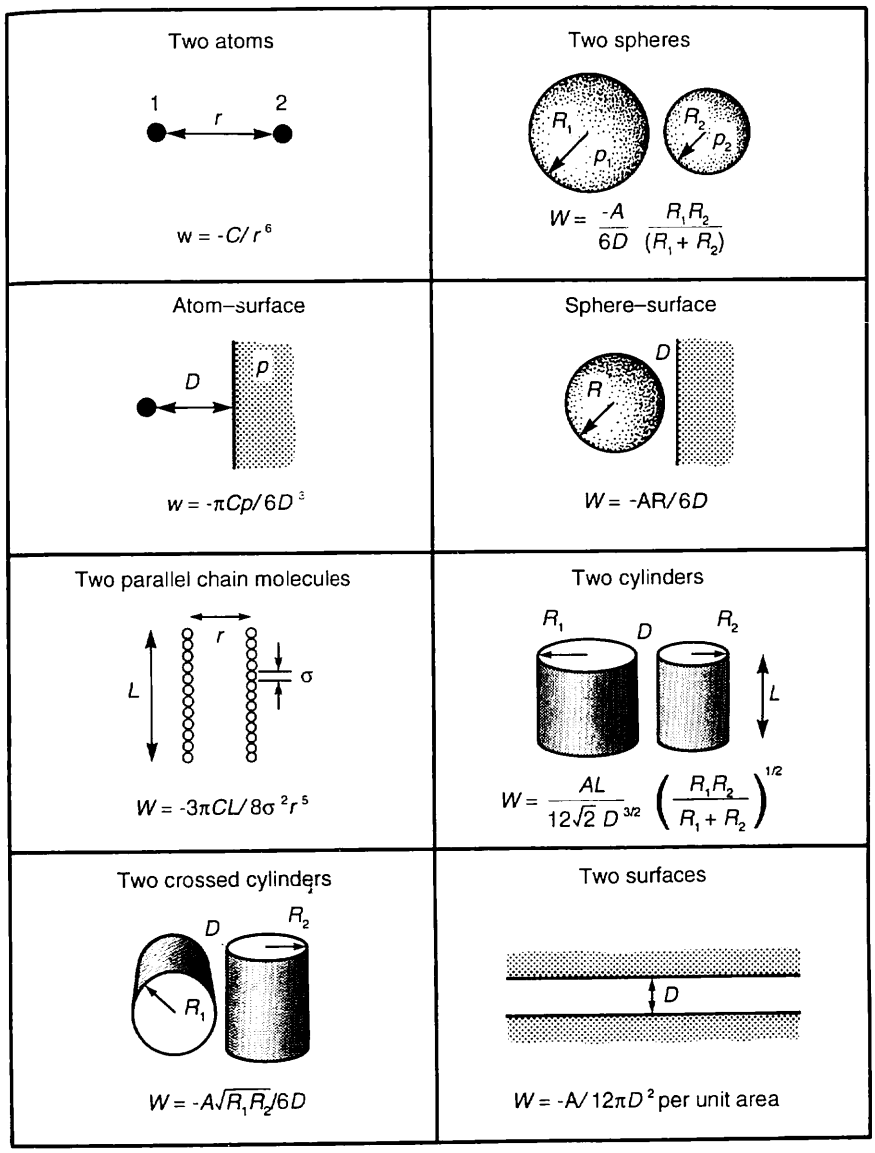

Fig. 11.1. Non-retarded van der Waals interaction free energies between bodies of different geometries calculated on the basis of pairwise additivity (Hamaker summation method). The *Hamaker constant* A is defined as $A = \pi^2 C\rho_1\rho_2$ where ρ_1 and ρ_2 are the number of atoms per unit volume in the two bodies and C is the coefficient in the atom–atom pair potential (top left). A more rigorous method of calculating the Hamaker constant in terms of the macroscopic properties of the media is given in Section 11.3. The forces are obtained by differentiating the energies with respect to distance.

if each body is composed of atoms for which $C = 10^{-77}\,\mathrm{J\,m^6}$ (cf. Table 6.1) and of number density $\rho = 3 \times 10^{28}\,\mathrm{m^{-3}}$ (corresponding to atoms of radius ~ 0.2 nm), the Hamaker constant is

$$A = \pi^2 10^{-77}(3 \times 10^{28})^2 \approx 10^{-19}\,\mathrm{J}\ (10^{-12}\,\mathrm{erg}).$$

Let us consider three cases more specifically. First, for hydrocarbons, treating them as an assembly of CH_2 groups, we have $C \approx 5 \times 10^{-78}\,\mathrm{J\,m^6}$ and $\rho = 3.3 \times 10^{28}\,\mathrm{m^{-3}}$ per CH_2 group, from which we obtain $A \approx 5 \times 10^{-20}\,\mathrm{J}$. This is shown in Table 11.1 together with similarly calculated estimates for carbon tetrachloride and water.

TABLE 11.1 Hamaker constants determined from pairwise additivity. Eq. (11.1).

Medium	C ($10^{-79}\,\mathrm{J\,m^6}$)	ρ ($10^{28}\,\mathrm{m^{-3}}$)	A ($10^{-19}\,\mathrm{J}$)
Hydrocarbon	50	3.3	0.5
CCl_4	1500	0.6	0.5
H_2O	140	3.3	1.5

Note that all three Hamaker constants are similar even though the media are composed of molecules differing greatly in polarizability and size. This is not a coincidence. It arises because the coefficient C in the interatomic pair potential is roughly proportional to the square of the polarizability α, which in turn is roughly proportional to the volume v of an atom (Section 5.1). And since $\rho \propto 1/v$ we see that $A \propto C\rho^2 \propto \alpha^2\rho^2 \propto v^2/v^2 \propto constant$. Of course, this is a gross oversimplification; nevertheless, the Hamaker constants of most condensed phases are found to lie in the range $(0.4\text{–}4)10^{-19}\,\mathrm{J}$.

11.2 STRENGTH OF VAN DER WAALS FORCES BETWEEN BODIES IN VACUUM OR AIR

Taking $A = 10^{-19}\,\mathrm{J}$ as a typical value, we can now estimate the strength of the van der Waals interaction between macroscopic bodies in vacuum (or air). Thus, for two spheres of radius $R = 1\,\mathrm{cm} = 10^{-2}\,\mathrm{m}$ in contact at $D \approx 0.2$ nm, their adhesion force will be

$$F = AR/12D^2 = (10^{-19} \times 10^{-2})/12(2 \times 10^{-10})^2$$
$$= 2 \times 10^{-3}\,\mathrm{N}\ (\text{or } 0.2\,\mathrm{g}),$$

while at $D = 10\,\text{nm}$ the force will have fallen by a factor of 2500 to about $10^{-6}\,\text{N}$, or 0.1 mg. Note that these forces are easily measurable using conventional methods.

Turning now to the interaction *energy*, at $D = 10\,\text{nm}$ the energy is $-AR/12D \approx -10^{-14}\,\text{J}$, or about $2 \times 10^6\,kT$, and even for particles with radii as small as $R = 20\,\text{nm}$ their energy exceeds kT at $D = 10\,\text{nm}$.

For two planar surfaces in contact ($D \approx 0.2\,\text{nm}$), the adhesive pressure will be

$$P = A/6\pi D^3 \approx 7 \times 10^8\,\text{N m}^{-2} \approx 7000\,\text{atm},$$

while at $D = 10\,\text{nm}$ the pressure is reduced by a factor of about 10^5 to a still-significant 0.05 atm. At contact the *adhesion energy* will be $-A/12\pi D^2 \approx -66\,\text{mJ m}^{-2}$, which corresponds to a surface energy of $\gamma = 33\,\text{mJ m}^{-2}$. This is exactly of the order expected for the surface energies and tensions of van der Waals solids and liquids, discussed later. We see, therefore, that the van der Waals interaction between macroscopic particles and surfaces is large, and not only when the bodies are in contact. Later we shall see that in a medium the interaction strength is reduced by about an order of magnitude, and that under certain conditions it can become repulsive.

11.3 THE LIFSHITZ THEORY OF VAN DER WAALS FORCES

The assumptions of simple pairwise additivity inherent in the formulae of Fig. 11.1 and the definition of A of Eq. (11.1) ignore the influence of neighbouring atoms on the interaction between any pair of atoms. First, as we saw in Section 5.7 the effective polarizability of an atom changes when it is surrounded by other atoms. Second, recalling our earlier simple model of the dispersion interaction between two Bohr atoms 1 and 2, if a third atom 3 is present, it too will be polarized by the instantaneous field of atom 1, and its induced dipole field will also act on atom 2. Thus, the field from atom 1 reaches atom 2 both directly and by reflection from atom 3. The existence of multiple reflections and the extra force terms to which they give rise is a further instance where straightforward additivity breaks down, and the matter becomes very complicated when many atoms are present (see Problem 6.2). In rarefied media (gases) these effects are small, and the assumptions of additivity hold, but this is not the case for condensed media. Further, the additivity approach cannot be readily extended to bodies interacting in a medium.

The problem of additivity is completely avoided in the *Lifshitz theory*